# Test Plan

Open-Source Laboratory Upgrade Point Absorber (LUPA) WEC Flume Testing for System Identification and Experimental Uncertainty

Awardee: Oregon State University

Awardee point of contact: Bryson Robertson

Facility: O.H. Hinsdale Wave Research Laboratory and Sandia National Labs

Facility Point of Contact:
Bret Bosma (O.H. Hinsdale) and Ryan Coe (Sandia)

Date: 2/3/25

TEAMER
Testing & Expertise for Marine Energy

# EXECUTIVE SUMMARY

The LUPA is a two-body point absorber WEC consisting of a surface float, which is primarily buoyancy driven, and spar reaction heave plate. It has a highly controllable power-take-off (PTO) that utilizes the relative motion between the float and heave plate and a linear-to- rotary mechanical system to drive the on-board generator. The LUPA was designed to be an open-source wave energy converter with modular components for experimental validation of hydrodynamic models, control systems, PTO designs, and hull and heave plate geometries. It has three modes of operation that allow for varying complexity: 1) A single float, heaving WEC; 2) A two-body, heaving WEC; and 3) A two-body, six degree-of-freedom WEC.

Many metrics frequently used in wave energy literature inherently include significant *uncertainty* (e.g. Capture Width Ratio CWR) yet are generally reported and published as single absolute variables. Utilizing the CWR example, the incident wave energy denominator is subject to significant uncertainty and dependence on WEC shape and wave characteristics. Uncertainty in wave energy testing measurements is underexplored and, once validated, the LUPA provides a great opportunity to quantify some of these uncertainties. LUPA exists to accelerate the development of wave energy by sharing lessons learned and detailing the process for testing wave energy devices, which are often underreported. Also, through large-sized WEC experimental testing, LUPA will provide a valuable open-source experimental and numerical dataset - which is lacking in the industry now.

# 1 INTRODUCTION TO THE PROJECT

The intended outcomes of testing the LUPA include validating numerical models, refining hydrodynamic coefficients, and quantifying uncertainty in WEC performance metrics – across three LUPA operating modes. In addition to this, the *process* used to complete the LUPA system identification and uncertainty will be well documented and shared with the wave energy community to improve understanding of uncertainty in WEC testing.

# 2 ROLES AND RESPONSIBILITIES OF PROJECT PARTICIPANTS

## 2.1 APPLICANT RESPONSIBILITIES AND TASKS PERFORMED

Researchers from Oregon State University (OSU) will lead experimental testing and data analysis.

Dr. Bryson Robertson and PhD Candidate Courtney Beringer will be responsible for:

- Ensuring LUPA design and build is complete, and ready for testing
- Conducting experiments in coordination with Sandia National Laboratories (SNL) and Hinsdale participants
- Post-processing all experimental campaign data and writing the post-access report.

## 2.2 NETWORK FACILITY RESPONSIBILITIES AND TASKS PERFORMED

Researchers from SNL will support system identification and uncertainty analysis, while the O.H. Hinsdale Wave Research Laboratory (Hinsdale) will support experimental testing in the Large Wave Flume. This includes the identification of relevant tank test trials (Hinsdale, applicant, & SNL co-lead), wave conditions (Hinsdale & applicant lead, SNL support), theoretical considerations for uncertainty analyses (SNL lead, Hinsdale and applicant support), and best practices for data analysis (SNL lead, Hinsdale and applicant support).

# 3 PROJECT OBJECTIVES

1) **System identification for multi-degree of freedom wave energy converters** – This project will build on existing experience for performing system identification tests on multi-degree of freedom wave energy converters [1]–[3] to further explore this important process for obtaining empirical models. As part of Objective (1), we will be investigating impedance matching feedback controllers. Previous work on designing, implementing, and assessing the performance of impedance matching feedback controllers will be performed [3]–[9].
2) **Uncertainty in estimation for wave energy converter performance metrics** – Experimentally based results for power generation, capture width, wave-to-wire efficiency, and wave power are all subject to uncertainties arising from finite accuracy and precision in measurements and experimental execution (e.g., wave maker repeatability). Additionally, model uncertainty may be important. Relatively little work has been performed in this area [10]–[14], but the importance of understanding

the uncertainty on these critical metrics cannot be overstated. Results from this objective will be relayed to active efforts on standards development (e.g., IEC) and experimental wave energy converter performance assessment (e.g., at WETS, PacWave, and EMEC). Note that detailed analysis of all the metrics within the IEC -100 standards and associated possible uncertainty analysis is beyond the scope and budget of this award. Within this project, findings for this testing will be presented to the relevant IEC standards committees.

# 4 Test Facility, Equipment, Software, and Technical Expertise

- **OH Hinsdale** - The O. H. Hinsdale Wave Research Laboratory has state of the art wave facilities and personnel with extensive experience testing wave energy devices. The LUPA was specifically designed to maximize the size, depth, and capabilities of the Large Wave Flume and was built on site. The Large Wave Flume (LWF) at Oregon State University's (OSU) O.H. Hinsdale Wave Research Laboratory (HWRL) in Corvallis, Oregon is 104 m in length, is 3.65 m wide, 4.57 m high and has a maximum water depth of 4 m. The flume has two wave makers: 1) a hydraulically actuated piston type wave maker, capable of making large-scale regular, irregular, Tsunami, and user defined waves in the range of periods from 0.8 to 12 seconds at a maximum depth of 2.74 m, and 2) an electrically actuated removable elevated-hinge flap-type wave maker, capable of making mid-scale regular, irregular and user defined waves in a typical range of periods from 0.5 to 4 s. The Large Wave Flume has a carriage for personnel access to instrumentation as well as an overhead gantry crane. Details of the Large Wave Flume and instrumentation available from HWRL can be found here: https://engineering.oregonstate.edu/facilities/wave-lab/facilities/large-wave-flume.
- **Sandia National Labs** – Sandia has extensive expertise in design, modeling, control, and testing of wave energy converters. Specifically, Sandia has performed and supported many wave tank tests (see, e.g., [1-9]) in which system identification and power maximizing control were implemented.

# 5 Test or Analysis Article Description

- **Test article description -** The LUPA WEC is a point absorber style WEC with three operational configurations: 1) A single float, heaving WEC; 2) A two-body, heaving WEC; and 3) A two-body, six degree-of-freedom WEC. Note that the single float, heaving WEC configuration will utilize the full heave plate with buoyancy floats – which will simply be locked in place to limit movement.

The LUPA resource database consists of a physical scaled WEC model (nominally 1:20 size – details shown in Figure 1 below), a scaled numerical WEC model, and the full-scale numerical WEC model.

*Table. LUPA Physical Specifications*

| Specification | Value | Units |
|---|---|---|
| Scale | 1/20 | m/m |
| Float Diameter | 1 | m |
| Total height | 3.7 | m |
| PTO Stroke Length | 0.5 | m |
| Mass | 436 | kg |
| Motor Continuous Torque | 46 | Nm |
| Water Depth | 2.7 | m |

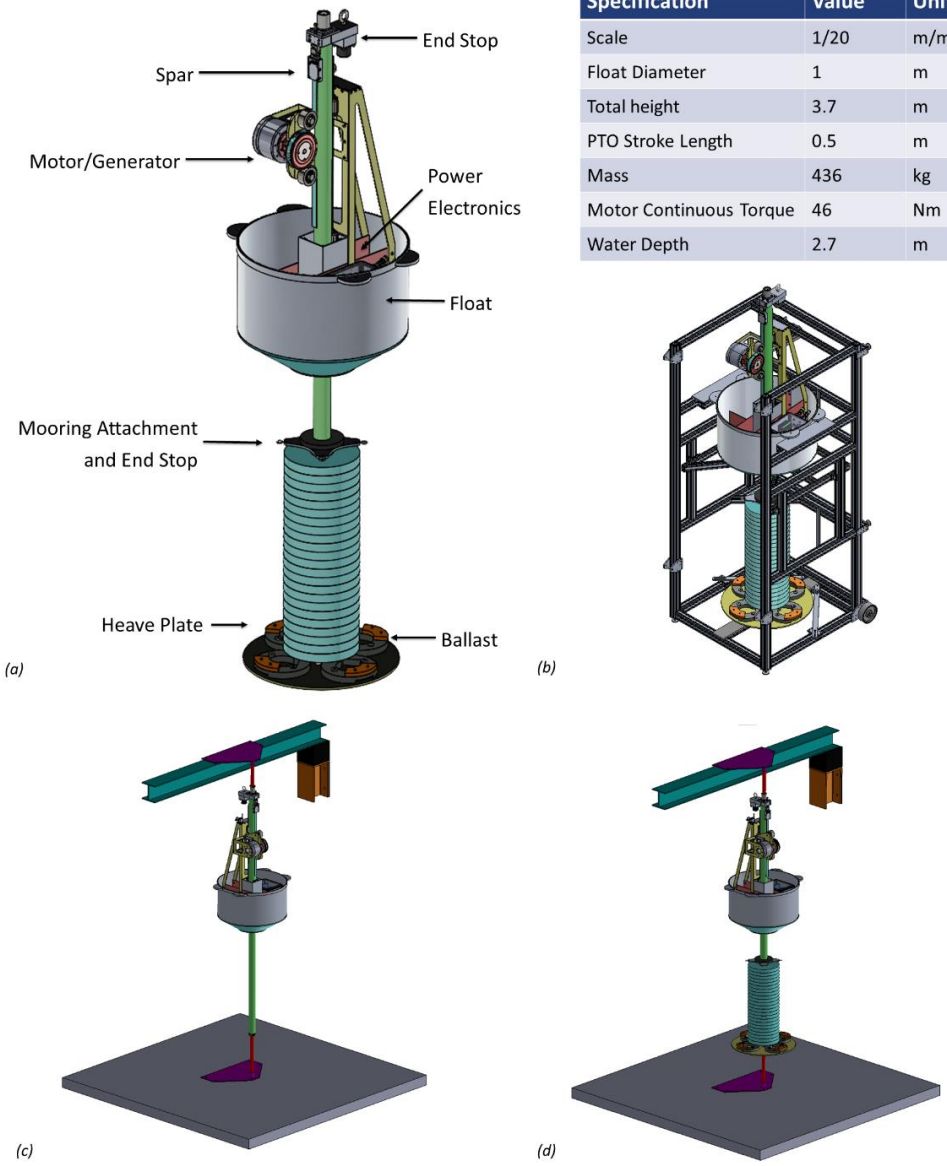


*Figure 1: a) Major components of the LUPA device. The six degree of freedom configuration utilizes a mooring set-up in the LWF. (b) Cradle for LUPA assembly, deployment and recovery. (c) Single-body, heave-only configuration. (d) Two-body, heave-only configuration. Note the height in the Table is the total height of the device, and the noted water depth is the minimum operational depth.*

- The numerical WEC models are developed in both WEC-Sim. The three operational configurations of LUPA, details on WEC parts, and physical specifications are detailed in Figure 1. LUPA consists of two hydrodynamically active rigid bodies – a surface following float, and a hydrodynamically stable heave plate. When introduced to incoming waves, the float will be excited and attempt to 'follow' the water surface, while the heave plate is located at depth in more quiescent water and will remain more static. A Power Take Off (PTO) system harnesses the relative motion between

the float and the heave plate to generate electrical power; through a linear displacement to rotary motion conversion (belt driven).

- **Intended purpose –** The LUPA was designed to be an open-source wave energy converter with modular components for experimental validation of hydrodynamic models, control systems, PTO designs, and float and heave plate geometries.
- **Advance marine energy technologies –** In this testing campaign, LUPA serves as a platform to study system identification of WECs and uncertainty of WEC evaluation metrics. These topics are important for advancing wave energy converter design, testing and survivability.

# 6 Work Plan

## 6.1 Experimental Setup, Data Acquisition System, and Instrumentation

- **Experimental Setup -** All testing will be conducted in the Large Wave Flume at Oregon State University's (OSU) O.H. Hinsdale Wave Research Laboratory (HWRL) in Corvallis, Oregon. The water depth of the experiments is 4.0 m. Scaling and wave conditions chosen for the LUPA are based on the PacWave test site, located off the coast of Newport, Oregon, USA. Froude scaling is used with a 1:20 model scale for the North and South sites, respectively. The LUPA has three modes of operation, with the setups shown in the Figure 1 above . LUPA has four taut mooring lines which are used in the two-body, heaving mode and the two-body, six degree-of-freedom mode. An initial setup is shown in the Figure 2 below. The LUPA is controlled in real time using MATLAB Simulink and a Speedgoat machine. Data is processed in real time and displayed for the user to monitor the WEC response and mechanical power production. This will be extended to model electrical power. Additional data analyses will be completed after testing to reduce the influence of noise and produce higher quality results.
- **Data Acquisition –** There are two data acquisition systems (DAQs) that are time synchronized: the Hinsdale DAQ and the onboard LUPA DAQ. The flow of power and data along with the sensors used onboard LUPA can be visualized in Figure 3. See Appendix A for a list of sensors and associated details.

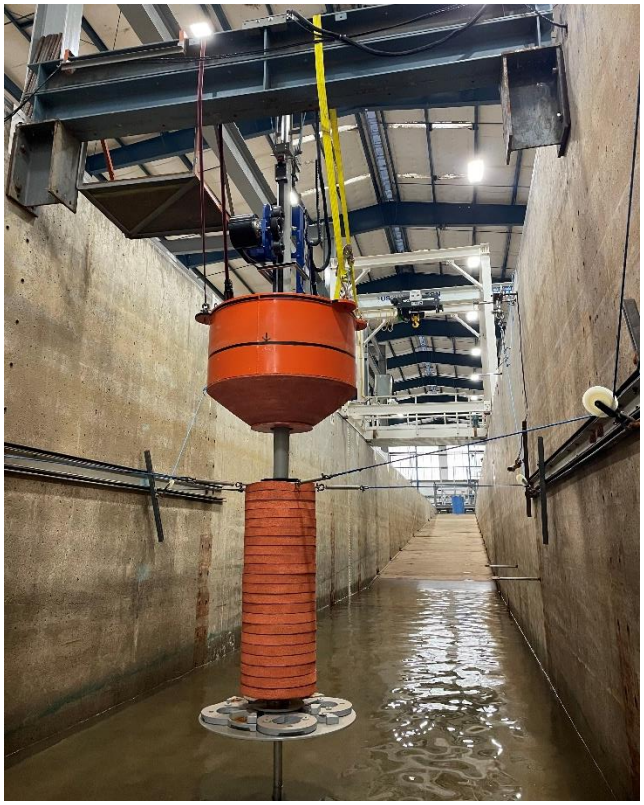

*Figure 2: The LUPA in the Large Wave Flume set up for mode 1 and 2 of testing. The black line around the float represents draft of the LUPA when floating under no waves.*

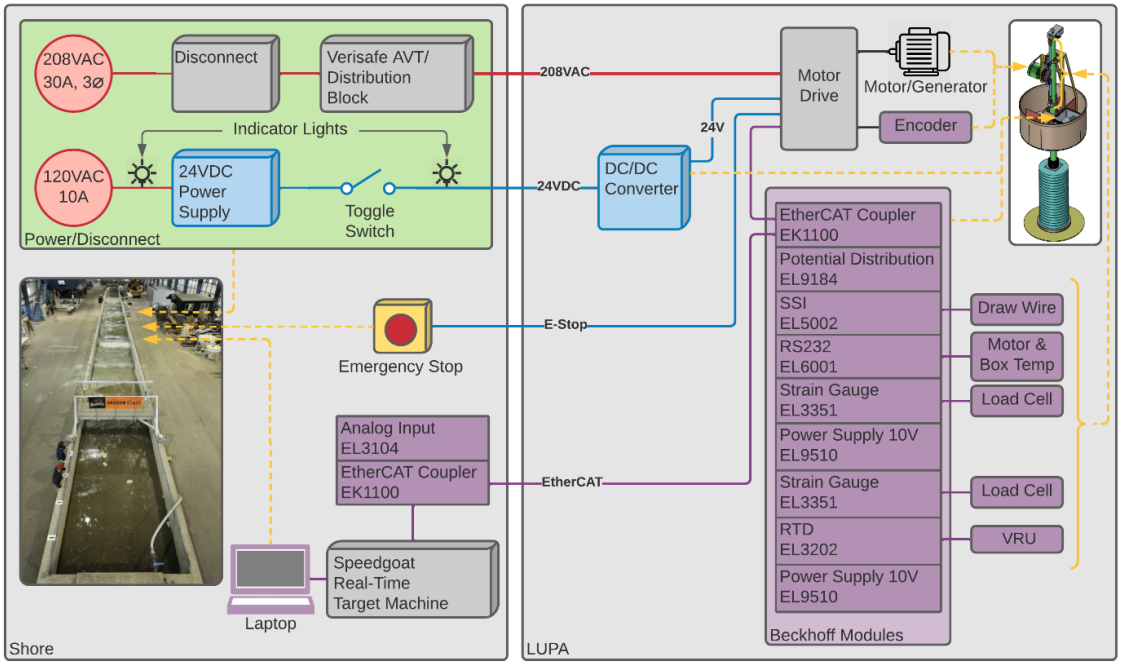


*Figure 3: Experimental setup for power and data*

## 6.2 Numerical Model Description

- **Simulation tool –** WEC-Sim has been used to perform initial validation and aide in the design of LUPA. Mesh studies and stability analysis where also performed. A damping optimization campaign was performed in WEC-Sim which will be verified through experimental testing. Boundary element method coefficients were obtained from WAMIT from numerical modeling and will be verified experimentally.

## 6.3 Test and Analysis Matrix and Schedule

The testing campaign is outlined below for the three testing objectives – which will be repeated for each operating mode of LUPA. Testing will occur from October 2nd to October 20th, 2023.

- **System ID –** The tests to perform a system identification include pink and white noise motor input in quiescent water and pink noise motor input with pink noise wave input. The motor signals and wave signals will be combined as necessary to understand the system. Gains on the motor signal will be used to achieve a wider range of conditions. These signals are shown in the two tables below.

*Table I: Motor multi-sine inputs*

| Test Condition | Motor Frequency Range | Phase Seed |
|---|---|---|
| **Pink 1** | Pink noise 0.05-2 Hz | 1 |
| **Pink 2** | Pink noise 0.05-2 Hz | 2 |
| **Pink 3** | Pink noise 0.05-2 Hz | 3 |
| **White 1** | White noise 0.05-2 Hz | 1 |
| **White 2** | White noise 0.05-2 Hz | 2 |
| **White 3** | White noise 0.05-2 Hz | 3 |

*Table II: Pink noise wave conditions with a frequency range from 0.05-1.5 Hz*

| Phase Seed | H = 0.1 m | H = 0.15 m | H = 0.20 m |
|---|---|---|---|
| **1** | Pink1A | Pink1B | Pink1C |
| **2** | Pink2A | Pink2B | Pink2C |
| **3** | Pink3A | Pink3B | Pink3C |

- **Uncertainty –** The uncertainty process itself informs the wave conditions. The operational range for the LUPA in regular waves at prototype scale is approximately H = 1 – 5 m, T = 7.5 – 25 s. For irregular waves (Pierson-Moskowitz), $H_s$ = 1- 5.2 m, $T_p$ = 7.4 – 15.5 s. The model scale wave conditions are in the tables below. Both regular and irregular wave conditions will be tested with multiple repeat periods, and be conducted at these three (3) times to assist in the identification of uncertainty within the same conditions. This approach allows for noise reduction and provide an opportunity from which uncertainty estimates may be made.

*Table III: Regular wave conditions*

| Wave Period (s) | H = 0.1 m | H = 0.15 m | H = 0.20 m |
|---|---|---|---|
| **1.0** | R1A | R1B | R1C |
| **1.5** | R2A | R2B | R2C |
| **2.0** | R3A | R3B | R3C |
| **2.5** | R4A | R4B | R4C |
| **3.0** | R5A | R5B | R5C |
| **3.5** | R6A | R6B | R6C |
| **4.0** | R7A | R7B | R7C |
| **5.0** | R8A | R8B | R8C |

*Table IV: Irregular wave conditions, Pierson-Moskowitz*

| Peak Wave Period (s) | $H_{m0}$ = 0.04 m | $H_{m0}$ = 0.07 m | $H_{m0}$ = 0.13 m | $H_{m0}$ = 0.21 m |
|---|---|---|---|---|
| **1.48** | P1A | P1B | P1C | P1D |
| **1.90** | P2A | P2B | P2C | P2D |
| **2.35** | P3A | P3B | P3C | P3D |
| **3.09** | P4A | P4B | P4C | P4D |

- **Impedance matching –** Experimental impedance matching utilizes the data collected in the conditions run for system identification and uncertainty to design feedback controllers (see, e.g., [9]) – these conditions are covered in Table 3 and 4. As previously discussed, multiple repeat periods of both regular and irregular wave cases will be utilized for testing (tests completed within the 'Uncertainty' test objective test conditions noted above), providing an opportunity for noise cancelation in postprocessing. The resulting performance will be compared with analytic predications to verify implementation and validate dynamic models.

## 6.4 SAFETY

The applicant and OSU facility staff will follow all relevant safety procedures and protocols outlined in the HWRL Safety Plan 2021. This document describes the comprehensive and proactive safety plan in use at the O.H. Hinsdale Wave Research Laboratory (HWRL) at Oregon State University (OSU). The plan is built upon the principles of involvement, identification, rules, and training. The plan applies to anyone and everyone conducting work at the facility, including but not limited to faculty, instructors, post-docs, researchers, staff, and students, whether University employees or visitors.

The facility adheres to the University safety policy as described below. The policy requires everyone to follow safe working practices and procedures. It applies to all Oregon State University employees, students, and any other individuals conducting business on OSU property. The policy states the following:

*Effective management of health and safety at Oregon State University is fundamental to delivering excellence in research and teaching. Health and safety should be a concern to everyone since our mutual efforts and vigilance are necessary to eliminate incidents that result in personal injury and loss of property. The majority of injuries and property*

*loss are costly and preventable. Through the dedicated efforts of everyone involved, we can maintain a safe and healthy environment while accomplishing the mission of the University. Oregon State University will make reasonable efforts to provide a safe and healthful working environment for all employees, students and others who may utilize the University's facilities and grounds. All University departments/units will develop and implement safety policies and procedures that promote an injury free environment. Anyone engaged in University related activities must exercise personal responsibility and care to prevent injury and illness to themselves and others who may be affected by their acts or omissions. No person shall intentionally interfere with or misuse anything provided by the University in the interests of health and safety. Individuals are required to have the proper training for the safe operation and use of university facilities, equipment and supplies as well as animal handling. Faculty and staff administrators will be held accountable for fulfilling their safety responsibilities. Flagrant disregard of the University safety policies and procedures may result in disciplinary action. Priority should be given to safe working conditions and job safety practices in the planning, budgeting, direction and implementation of University activities. The OSU Health and Safety Policy should be read in conjunction with SAF 103: OSU Safety Program and other safety policies contained in the OSU Safety (SAF) Policy and Procedure Manual.*

All visitors, researchers and clients performing an activity within HWRL will undergo a specific and documented Safety Training, reviewing general safety procedures, rules and hazards. Temporary visitors will use yellow safety vests for best identification and awareness, and should use safety shoes at all times while working on the laboratory floor. Other safety protocols will be reviewed with the client during the Safety Training.

Safety Briefings will be performed at the beginning of the project and every time a safety hazard or activity is identified. HWRL staff and visitors are required to attend each and every briefing.

## 6.5 Contingency Plans

At this stage of the development pathway for LUPA, there are limited risks or need for significant contingency plans. The largest possible risk is lack of access to the O.H. Hinsdale Wave Research Laboratory, which will be managed by direct and constant communication with Dr. Pedro Lomonaco (Hinsdale Director).

## 6.6 Data Management, Processing, and Analysis

### 6.6.1 Data Management

- Data is to be stored locally at OSU and on hard drive backup. Raw and processed data will additionally be compressed and zipped onto Box. A ReadMe file for the data describing the data will be included with all data files. Processing of data will be conducted at OSU the day following a drain calibration of wave gauges.
- OSU has a server that will house the data on their end. They also will have a hard drive backup. At the end of the project, they will lock the directory and archive it (read only). Raw data file and raw data in engineering units will be transferred to MHK DR and then processed on site the following day.
- Raw Data: Surface elevation at wave gauge locations.
- Processed Data: Free surface elevations, wave height, wave period.

- Raw data path:

1. Recorded locally on each individual DAQ hardware component (PXI system). All filenames include a timestamp off a PTP (IEEE-1588) synchronized clock, so there's no possibility of accidental overwrites. After each trial is completed, every data file is pushed on to step (2).
2. Recorded locally on the DAQprocessor (Mac mini). This is continuously backed up to an external drive (macOS Time Machine). It's not running any services other than accepting inbound connections from the PXI systems to dump data. When each file arrives, it is evaluated and then placed on depot (step (3)) in the correct project, experiment, and trial. Data is put in the DAQprocessor trash after each project is completed, and then erased a month later. The backups persist for years.
3. Stored on the depot file server. This is also where the path for everything BUT raw data (intermediate data, code, photos, videos) forks in. Depot has an hourly snapshot backup system, so if something is deleted by accident it can be recovered immediately. More here:https://it.engineering.oregonstate.edu/restore-using-snapshots
4. Archived on attic. This is not backed up by snapshots. Instead it's backed up by multiple hard drives, spread in different locations around the lab and around Corvallis at a radius on the scale of miles.

| Data to be submitted | Data types |
|---|---|
| motion capture data | ASCII logs and plots |
| video data | video files |
| power production data and drive train data | ASCII logs and plots |
| wave data | ASCII logs and plots |

### 6.6.2 Data Processing

Data will be processed using MATLAB code at OSU by the applicant in between tests to enable quality assurance in the event of signal errors.

Data will be translated from analog voltages to engineering units following the last data collection or calibration event needed for the dataset. OSU Hinsdale staff is responsible for developing and updating the calibrations for Hinsdale equipment, while OSU students (Courtney Beringer - funded by NSF) will be responsible for LUPA instrumentation.

Uncertainty in measurements and WEC performance is a key research outcome of this testing campaign so due care will be taken to measure and collect data for all possible measurement uncertainties.

### 6.6.3 Data Analysis

Linear system identification methods will be applied following Pintelon and Schukens [15], building off previous applications for wave energy converters. Nonlinearity of the device will be assessed based on

comparing multiple linear models derived from different experiments (see, e.g., [3,15]) and by computing harmonic distortion. If necessary, multiple linear models may be derived to suit different operating regimes. Based on these models, linear feedback controllers will be designed to maximize power absorption/generation. Uncertainty in power absorption/generation, capture width, and wave-to-wire efficiency will be estimated using multiple methods, including analytic [16] and numerical ("Monte Carlo") propagation [13].

# 7 PROJECT OUTCOMES

## 7.1 RESULTS

These findings are the result of experimental testing of the Laboratory Upgrade Point Absorber (LUPA) at the O.H. Hinsdale Wave Research Laboratory Large Wave Flume at Oregon State University from October 30th, 2023, to November 8th, 2023. The two-body six degrees of freedom LUPA configuration was used for all tests to accomplish the goals of multi-degree of freedom (DOF) system identification (SI) and represent realistic conditions for uncertainty analysis.

Figure 4 below shows LUPA deployed in the flume with a wave test running. The water depth was constant for the entire testing campaign at 3.695 m. The results section is divided into two parts which match the project objectives: 1) System identification and 2) Uncertainty.

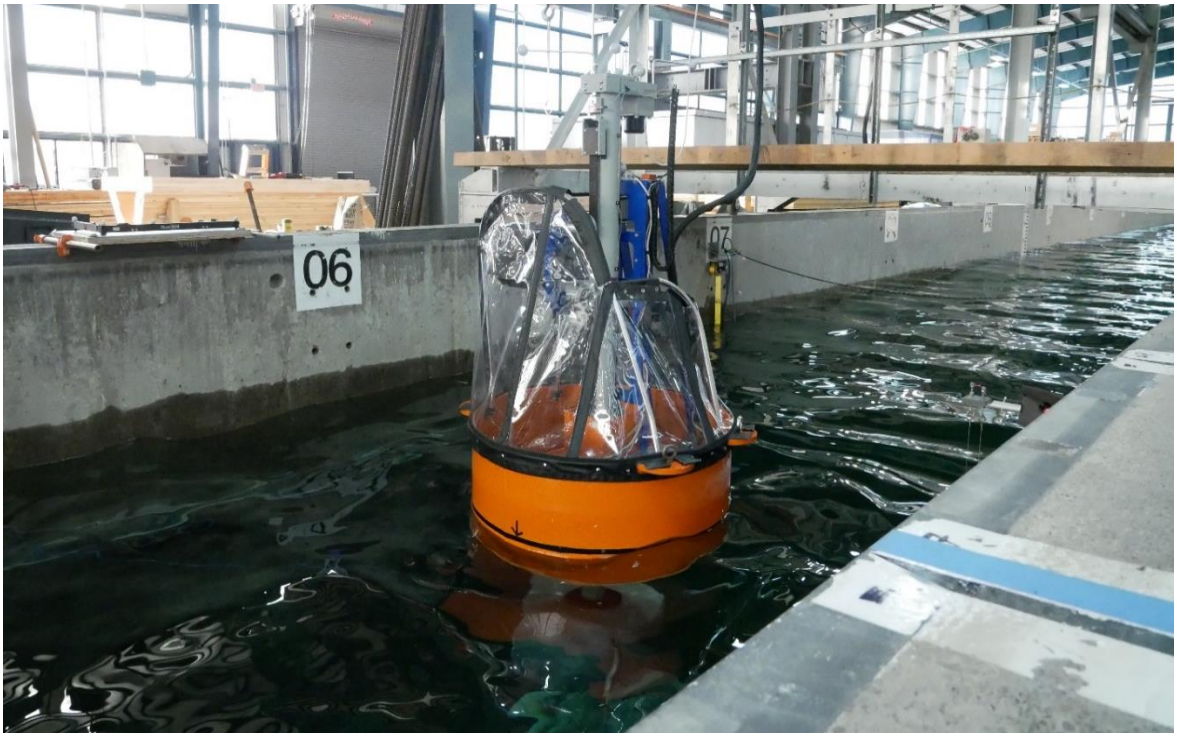


*Figure 4: LUPA deployed in the LWF undergoing a wave test. It is moored to the tank via springs in line to the yellow winch straps in the background.*

*System Identification*

We chose a single experimental dataset for the identification of both the excitation transfer function and the intrinsic admittance transfer function. We express both transfer functions relative to the PTO degree of freedom (DOF) and we chose to present them in a non-parametric form, due to their high order, which may be caused by the 6DOF motion of the system.

The single experiment contains 6 distinct trials to capture the response. These include two different amplitudes of white noise (WN) amplitude spectra for the implementation of the multisine (MS) PTO torque signal for forced oscillation (FO). For each input amplitude, we utilize three different phase realizations. The wave maker inputs are created from a pink noise (PN) amplitude spectrum with varied phase realizations. This experiment hierarchy is depicted in Table V.

*Table V: System Identification experiment hierarchy.*

| Pink Noise plus Force Oscillation (PNFO) Experiment | | | | | |
|---|---|---|---|---|---|
| Actuator torque amplitude = 3A | | | Actuator torque amplitude = 4.5A | | |
| Trial 1 | Trial 2 | Trial 3 | Trial 4 | Trial 5 | Trial 6 |
| PN wave 1 | PN wave 2 | PN wave 3 | PN wave 1 | PN wave 2 | PN wave 3 |
| MS FO 1, 3A | MS FO 2, 3A | MS FO 3, 3A | MS FO 1, 4.5A | MS FO 2, 4.5A | MS FO 3, 4.5A |

During each trial, the multisine signals used a repeat period of 5 minutes (300s) and were repeated a total of four times. In an idealized fashion, this sums up to a total experiment time of only 6 x 20 minutes = 2 hours to complete the SI. The authors would like to emphasize the marked efficiency of this approach to obtain both the system dynamics and the excitation characteristics in a mere 2 hours of experimental testing – these tasks are regularly allocated an entire week of time in many wave tank testing campaigns.

For the system identification, we choose a somewhat arbitrary offset from the beginning of each trial and then choose *exactly* $N_{rep} = 3$ full repeat periods (i.e., 900s worth of data). We present the entirety of data that goes into the system identification analysis in Figure 5. This figure shows six sets of time-domain recorded signals and their corresponding spectral content (evaluated at integer multiples of $N_{rep}$) below the respective time series.

Please note that the force signal (shown in yellow) are almost perfectly flat (“white”) spectra, indicating that the motor and drive perform exactly as intended. The wave input spectrum is noisier since the forced oscillation from LUPA also result in waves that superimpose on the wave maker’s input. The relative velocity spectral content looks fairly noisy, however, within each trial, the repeatability of the MSs was more than adequate to allow for a clean analysis (very low energy content in the components that are not integer multiples of the repeat period).

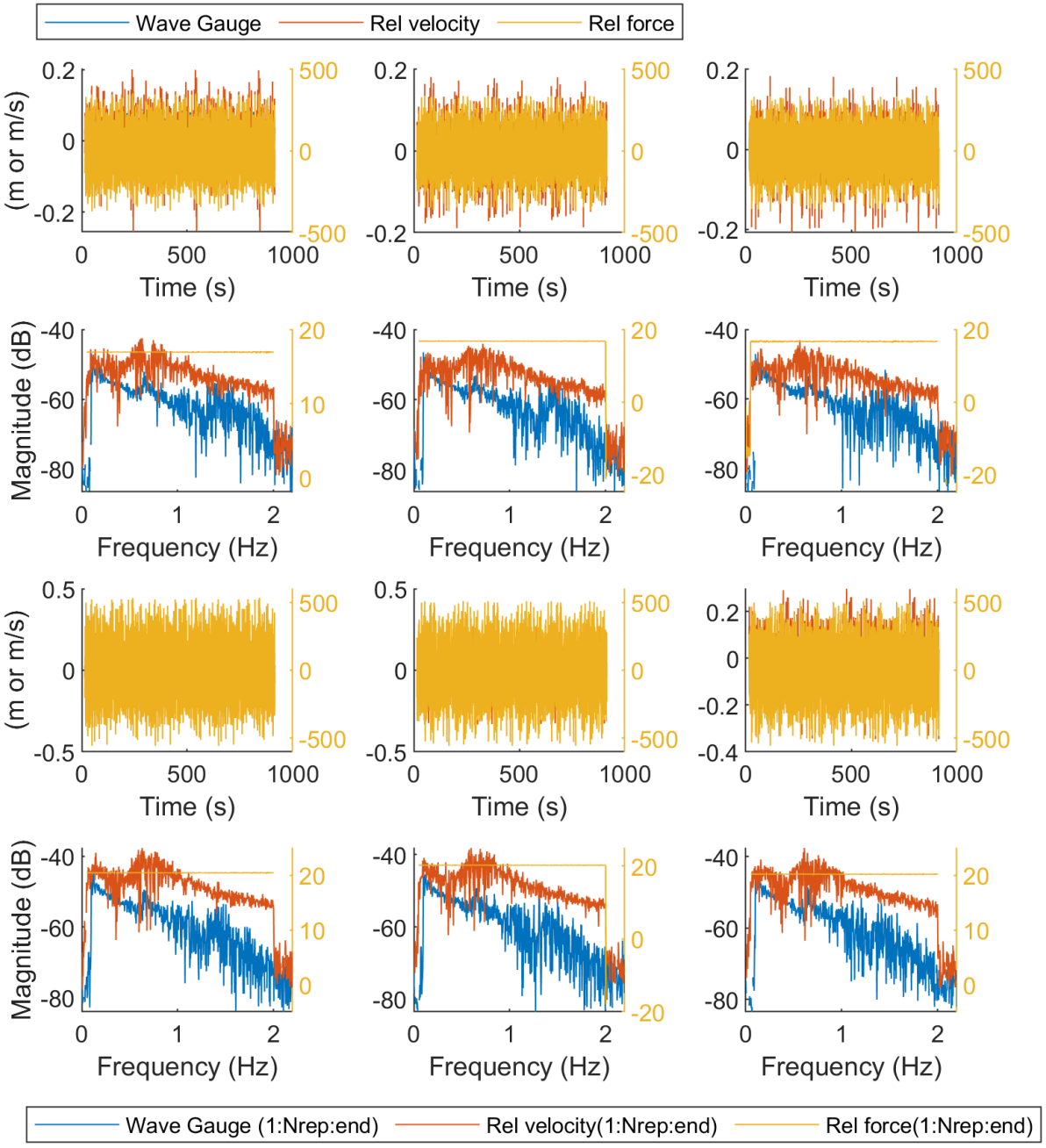


*Figure 5: System Identification Input Signals: Pink Noise wave input and Multi-Sine force input. Different trials are along the x-axis and the different experiments (MS amplitude) are in the rows.*

Consequently, the combination of the three phase realizations resulted in system models with high confidence. The results of the spectral analysis for both FO MS amplitudes are presented in Figure 6. The low confidence from wave to relative velocity above 1.3Hz can be explained with the poor signal to noise ration of wave and velocity (compare Figure 5.)

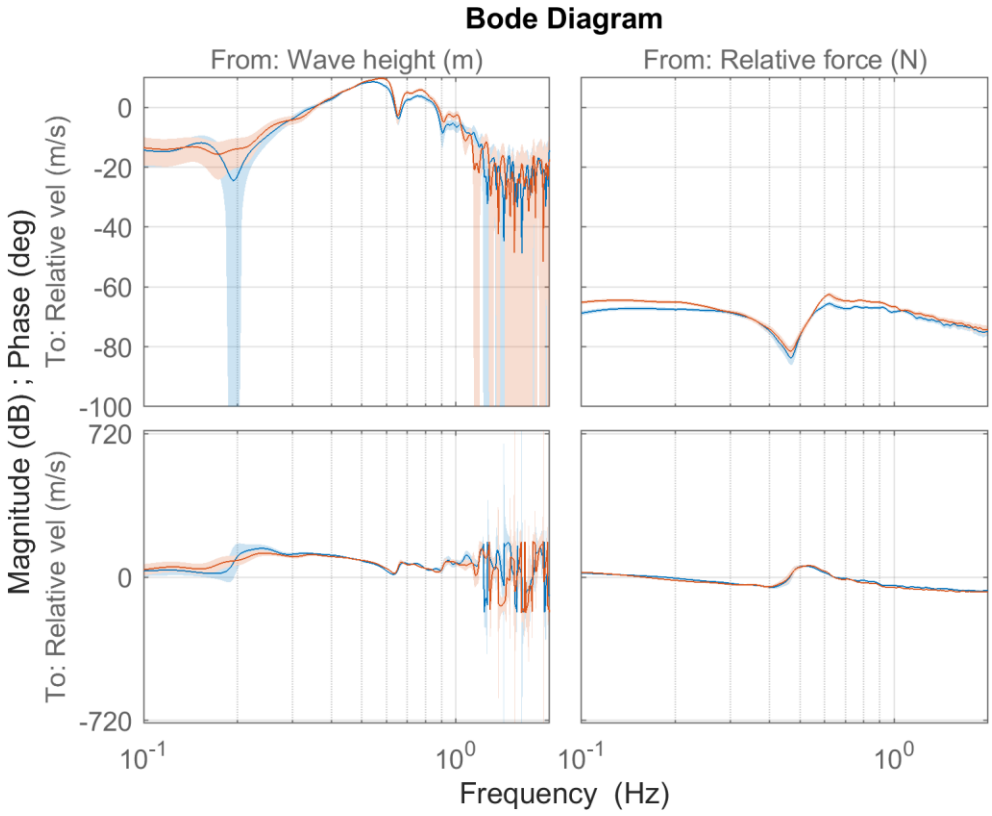


*Figure 6: LUPA 6 DOF MISO System ID non-parametric model results.*

The resulting non-parametric multiple input single output (MISO) model is the transfer function from wave height $\eta$ and relative force $F_{rel}$ to relative velocity, namely,

$$U_{rel} = [G_{11}\ G_{12}]\begin{bmatrix}\eta \\ F_{rel}\end{bmatrix}.$$

Here, the second element is equivalent the relative body equivalent intrinsic admittance,

$$Y_i = G_{12},$$

and we can further isolate the wave excitation force transfer function to the PTO,

$$H_{ex} = \frac{G_{11}}{Y_i} = \frac{G_{11}}{G_{12}}.$$

We illustrate those quantities more commonly used in the field of wave energy (the wave amplitude to excitation force transfer function and the intrinsic impedance) in Figure 7. A first good sign is that $H_{ex}$ is in good agreement for both amplitudes of forced oscillation tests (since it should be independent of the actuation). Further, please note the difference in magnitude of the intrinsic relative body admittance, which does show an amplitude dependency, suggesting nonlinearities and the need for multiple linear models describing the system at different operation amplitudes.

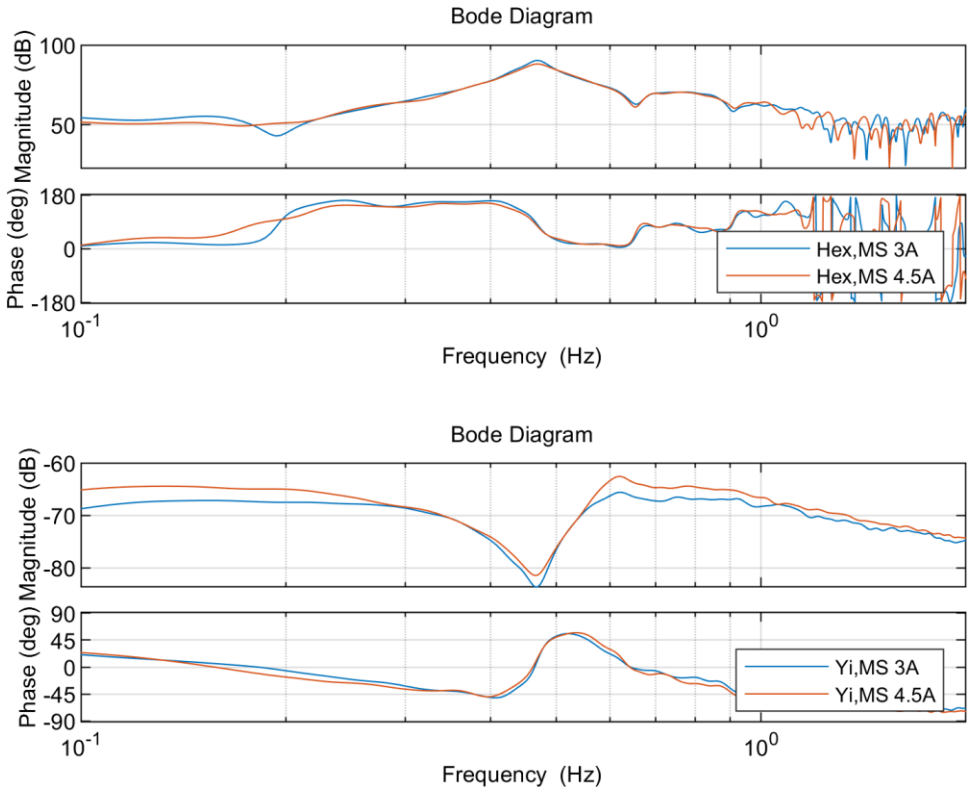


*Figure 7: LUPA 6DOF Excitation transfer function and intrinsic admittance.*

In the next section, we will go beyond visual analysis and perform a more rigorous validation of the obtained system models.

*System Identification Validation*

We chose two different experiments to validate the system identification results (and compare against Figure 6): First, a chirp input force signal with no waves and, second, a distinct PN wave and WN MS force which was not previously used for system identification.

The chirp validation results are plotted in Figure 8 and the MS results in Figure 9. In each figure, the top plot (a) contains the trimmed time domain signals which are analyzed. The next plot (b) is a Bode diagram of the spectral content of the measured signals (input and output) as well as the simulated output spectra for the two identified models from experiments employing an RMS input current level of 3A and 4.5A, respectively. It is interesting to note that natural frequency of the slosh waves that travel across the width flume at 0.65Hz (refer to Lesson Learned and Test Plan Deviation) is much more amplified with the chirp signal only. This can be explained by the circular radiation pattern of LUPA and that LUPA creates a standing wave that results in increased output velocity that is not obstructed by incoming waves from the wave maker.

As a first metric, we investigate the magnitude squared coherence between the input signals and the corresponding resulting velocity outputs. The coherence gives us insight about how well a linear model could describe the relationship between input and output at different frequencies.

For the chirp signal (Figure 8(c)) we can see that the relationship between relative force and relative is mostly linear across most frequencies (close to one) except for near 0.45Hz, which is the zero crossing of the relative body motion intrinsic admittance (see Figure 7) -- i.e. there is very little relative motion at this frequency, which is also observable around 1.5e4 samples in the time domain signal in subplot (a).

The nonlinear relationship is further amplified when waves are part of the experiment, as seen in subplot (c) of Figure 9 by the reduced average coherence compared to the chirp experiment. The output velocity observed in the pink noise waves plus forced oscillation experiment cannot be explained by either input signal alone, therefore we further present the coherence of the multi input single output (MISO) system. It is interesting to observe that a linear model never perfectly describes the relationship, but with 0.95 average coherence, comes very close.

Finally, let us investigate how well the obtained non-parametric models in Figure 6 can predict the observed response from the validation signals.

In the subplots (d), we present the error between the observed output spectra and the spectra that result from multiplying the input spectra by the system model transfer functions in Figure 6. If the spectra were to agree perfectly, we would see a magnitude and phase of zero in the Bode plot. Beyond the visual interpretation across the spectrum, we also compute the normalized root mean square error to quantify the goodness of the fit, given in the legend entries.

The biggest deviation for the chirp signal is at 0.65Hz (compare Figure 8 (d)), which is the reflection of the flume walls. It is in fact positive to see a mismatch between model and measured output here, since capturing the flume characteristics in the WEC model is not desirable. The goodness of the fit is 68.93% for the 4.5A model and 55.92% for the 3A model.

The validation experiment with pink noise waves and white noise forced oscillation is predicted fairly well across all frequencies. The model obtained for the 3A RMS white noise current spectrum fits better (71.89%) than the 4.5A (66.45%), which is not surprising, since the validation experiment was also conducted with 3A. This means that a simple non-parametric linear model can reproduce the complex multi DOF dynamics.

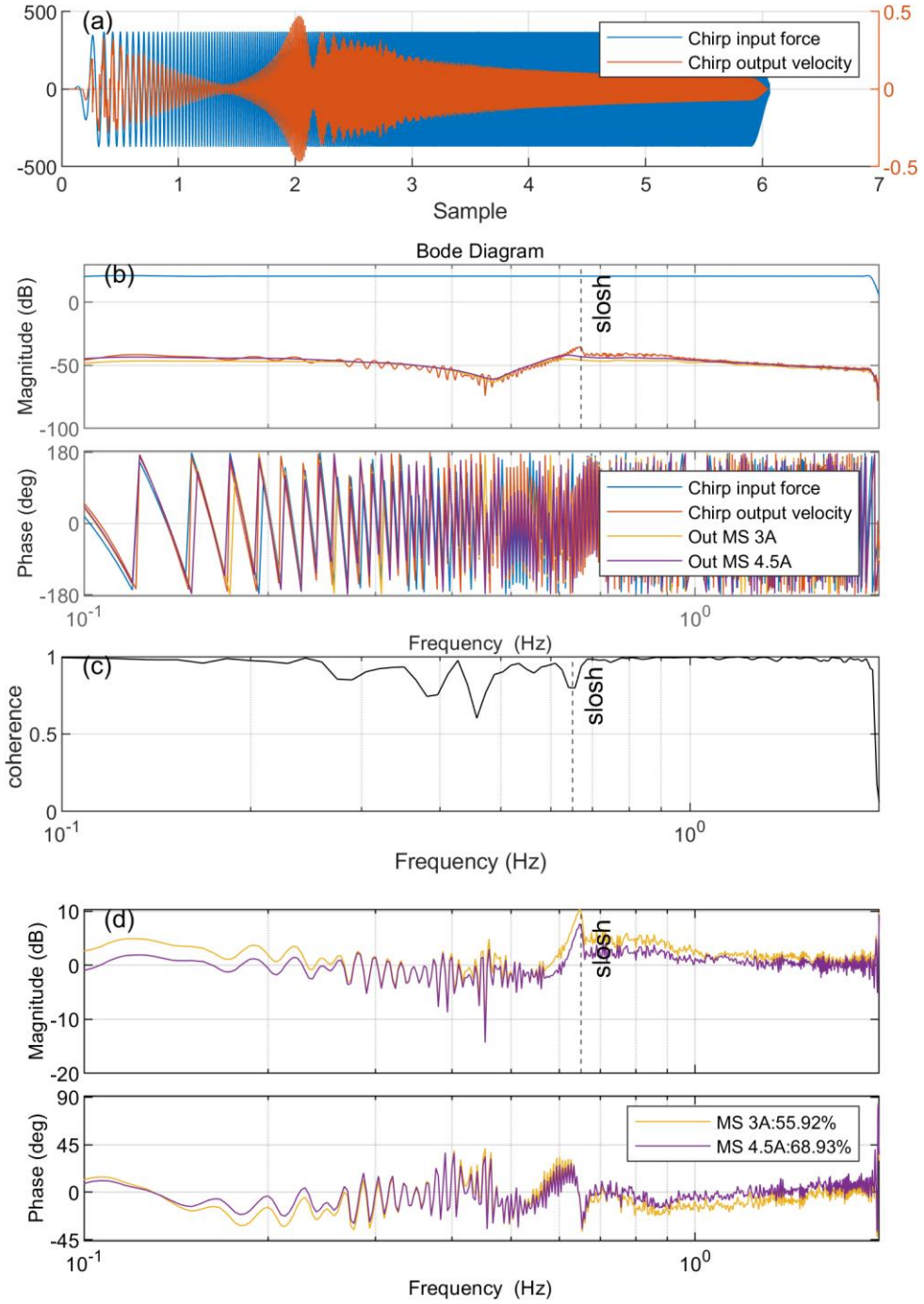


*Figure 8: Input and out comparison with a chirp input force signal and no waves. (a): Time domain signals, (b) frequency domain signals measured and simulated, (c) coherence of the measured input and out signals, (d) error between the measured and simulated output spectra.*

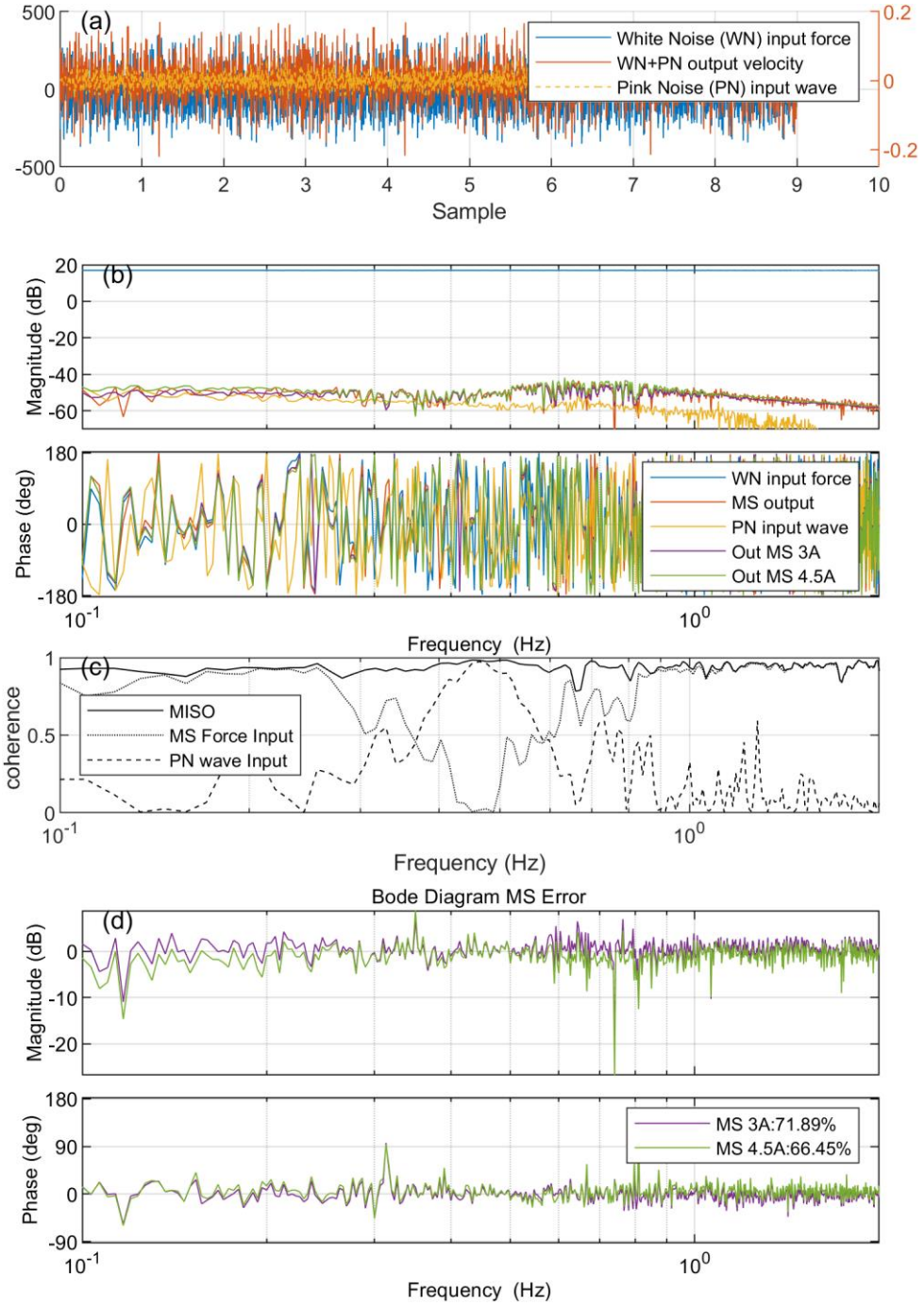


*Figure 9: Input and out comparison with a white noise input force signal and pink noise waves. (a): Time domain signals, (b) frequency domain signals measured and simulated, (c) coherence of the measured input and out signals, (d) error between the measured and simulated output spectra.*

*Uncertainty*

To address the objectives of uncertainty testing, detailed uncertainty analysis was completed on the LUPA experimental data collected in this campaign following the ITTC guidelines [17] and recommendations by Orphin et al. [14].

These results explore two main sources of uncertainty. First, *measurement uncertainty*, which is inherent in experimental testing as sensors and the environment are imperfect. Within *measurement uncertainty*, uncertainty is classified as aleatoric (type A) and epistemic (type B) uncertainties. These were found through repeat tests and sensor calibrations, respectively. Second, *nonlinear effect uncertainty,* deals with nonlinearities which exist in reality but often simplified down to their linear approximations. The nonlinear effects can be quantified by comparing the linear and nonlinear estimations of the wave energy flux.

Wave energy flux is an important parameter that defines the incident wave energy to a WEC device. It can also be used to define the efficiency of the WEC through the capture width ratio. The current IEC standards use a linear approximation of wave energy flux [18], which may underestimate the incident wave energy and be less accurate than the full nonlinear analytic solution [19], resulting in *nonlinear effect uncertainty*. The measurement uncertainty of wave energy flux and associated capture width ratio are not well explored in experimental tests.

Figure 10 shows wave elevation, $\eta(t)$, data collected by a wave gauge placed at the future location of LUPA in the flume. This data is referred to as "undisturbed hydro" testing as the LUPA WEC is not present in the tank. It is segmented by wave cycles and phase averaged. The figure shows some slight wave-to-wave variation in the peaks and troughs, which causes uncertainty in the calculated wave height and period. The requested wave height was 0.15 m, but the wave maker consistently produced a wave height around 0.13 m. The wave conditions are referenced regarding the requested conditions for consistency, but the actual measured average wave height is used in data analysis.

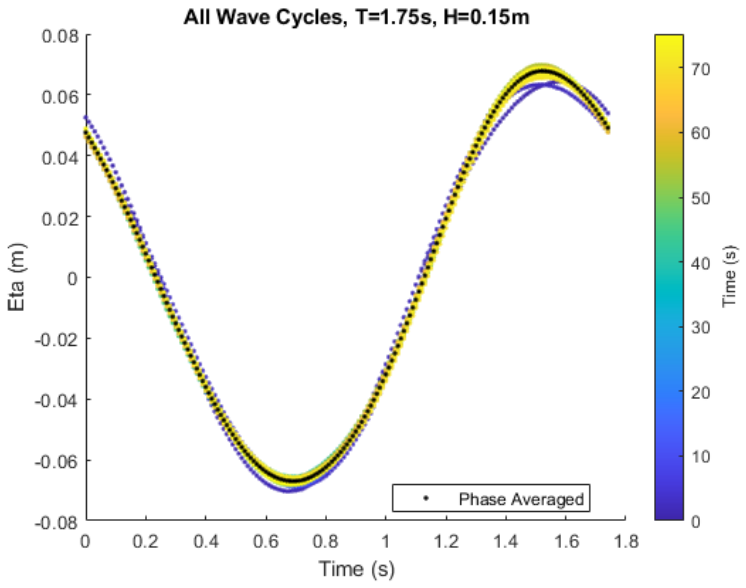


*Figure 10: Wave elevation data segmented by wave cycles and phase averaged. The x-axis is the phase time and the colorbar is the time since the first wave analyzed.*

Figure 11 and Figure 12 show the wave height and wave period type A standard uncertainty percent, respectively. The wave height and period uncertainty are below 0.4 % of the nominal value. The smallest wave height has the greatest uncertainty, likely due to the signal-to-noise ratio in the measurement signal. There is no significant difference in wave period uncertainty across the two periods tested. This is common as wavemakers are typically more accurate and consistent in generating wave periods than wave heights. The wave height type A uncertainty for the 0.15 m wave height is consistently higher than the Type A uncertainty for the 0.10 m wave height (at the 1.75 s wave period as shown in Figure 11). This is likely due to increasing nonlinear wave effects in larger wave heights.

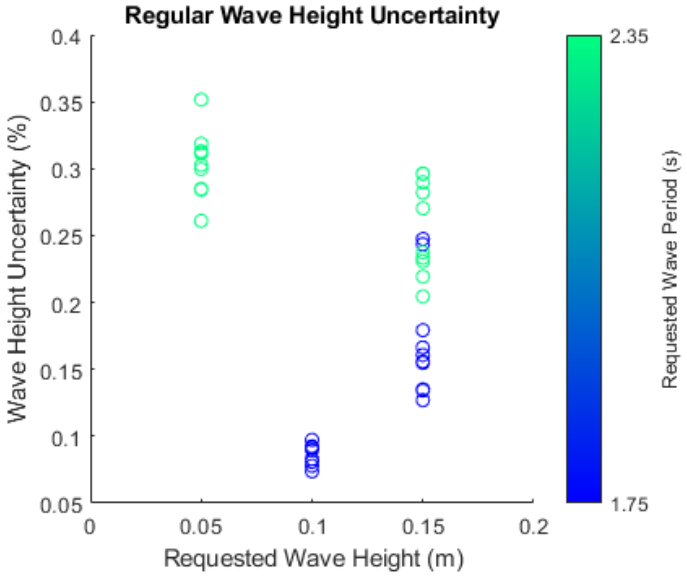


*Figure 11: Type A percent uncertainty of wave heights. Each circle represents a trial with at least 20 wave cycles.*

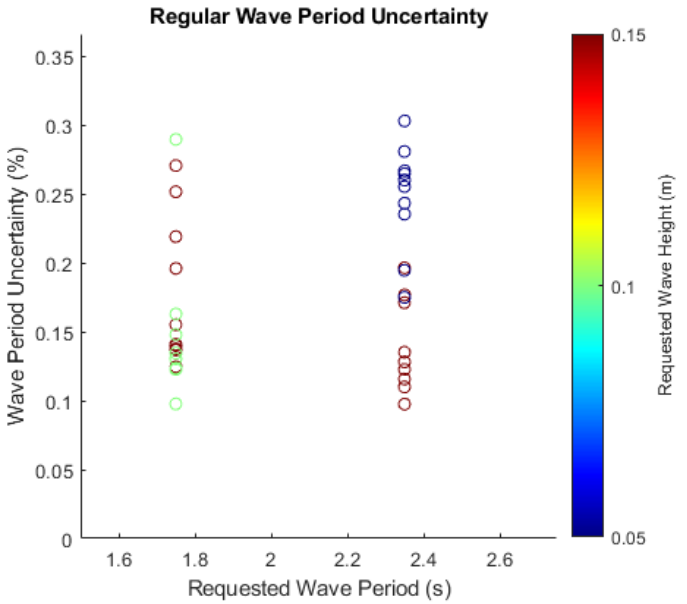


*Figure 12: Type A percent uncertainty of wave periods. Each circle represents a trial with at least 20 wave cycles.*

The IEC guidelines [20] indicate that special attention needs to be given to reflected waves in the testing environment. The impact of beach reflections is minimized by placing LUPA close to the wave maker and inducing breaking through the 1:12 beach slope. A reflection analysis is performed here as it pertains to uncertainty. The regular wave heights are measured over a single trial and an example is shown below in Figure 13 which separates data points between "with-reflection" and "without-reflection" as defined by the wave speed at the given period and the distance the wave travels to return to the wave gauge. The standard deviation of wave heights is similar between the with- and without-reflection for all the wave conditions tested, but the with-reflection data often have larger outliers. However, the uncertainty in wave heights is lower across all wave conditions when data *with* reflected waves is included. This is because uncertainty is inversely related to the number of samples. The number of samples without-reflection is 18 waves, but with-reflection the number of samples is 43.

Figure 14 shows the difference in type A uncertainty between with- and without-reflection data. These initial results show the potential benefits of running longer-duration trials: lower uncertainty and more efficient testing with less settling time.

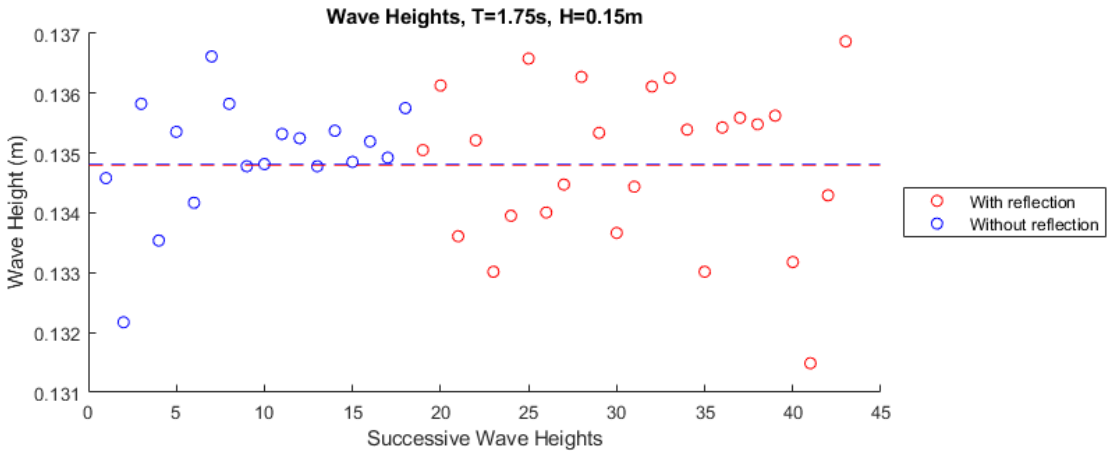


*Figure 13: Measured wave heights over a single trial with a programmed wave period of 1.75 s and a wave height of 0.15 m. The dotted lines are the mean of the with- and without- reflection.*

To find the expanded uncertainty with 95% confidence of incident wave power and understand the effects of uncertainty due to nonlinearities, the Monte Carlo Method was used to propagate uncertainties through both a linear and nonlinear estimation of incident wave power. The linear equation was taken from IEC specifications and the nonlinear equation was taken from Mohtat et al. [19]. The subject of this funding is not to complete a full uncertainty analysis, but rather to perform the experiments, thus a summary of the initial results is shown below. These plots and data are omitted from the MHKDR upload as the exact methods are still being developed and the results will be used in a journal publication. The data and processing codes will be released to MHKDR on the timeline of the journal publication.

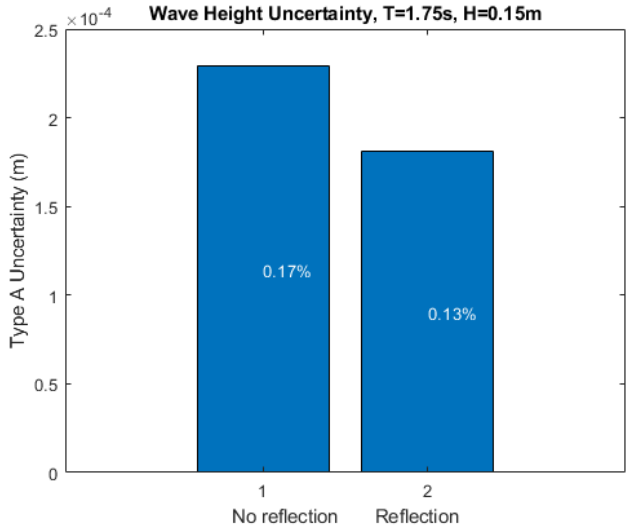


*Figure 14: Type A uncertainty in wave heights with and without reflection.*

Figure 15 shows the initial combined uncertainty results of the Monte Carlo simulation. The inputs to the Monte Carlo simulation are on the X-axis from left to right: gravity, water density, water depth, wave height, and wave period. The outputs continuing left to right are: group velocity, linear energy, nonlinear energy, linear power, and nonlinear power. These results show that there is more uncertainty in the case with lower wave steepness; likely due to the small wave height and associated signal to noise ratios in the data.

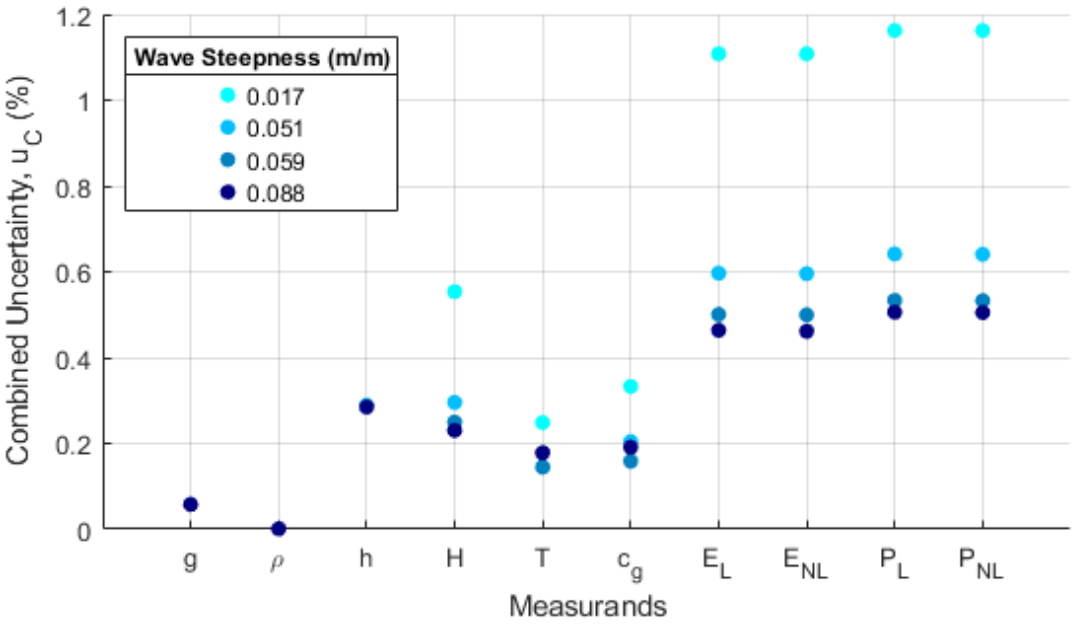


*Figure 15: Combined uncertainty of each Monte Carlo input and output across the four trials of varying wave steepness*

The linear and nonlinear energy and power uncertainty is very similar. In the experimental tests, the steepness is still relatively low compared to breaking waves (around 0.4) and the higher order terms are still very small. To test this theory, a Monte Carlo simulation was used to test a steeper, thus more nonlinear, wave condition, the results are shown in Figure 16. This result shows that with a very steep, nonlinear wave, the uncertainty in the nonlinear estimation is slightly higher than the linear estimation, but both are still under +/- 0.5% for wave power. This occurs because the higher order terms propagate the uncertainty due to wave height and also include the uncertainty of wave period and water depth (which the linear estimation does not consider). It is important to note that this wave condition was not physically run in the tank so the Type A uncertainty for wave height and period were applied as a mean of the tested conditions. The trend still stands but the magnitude of the uncertainty could be better understood with additional experimental testing of steeper waves.

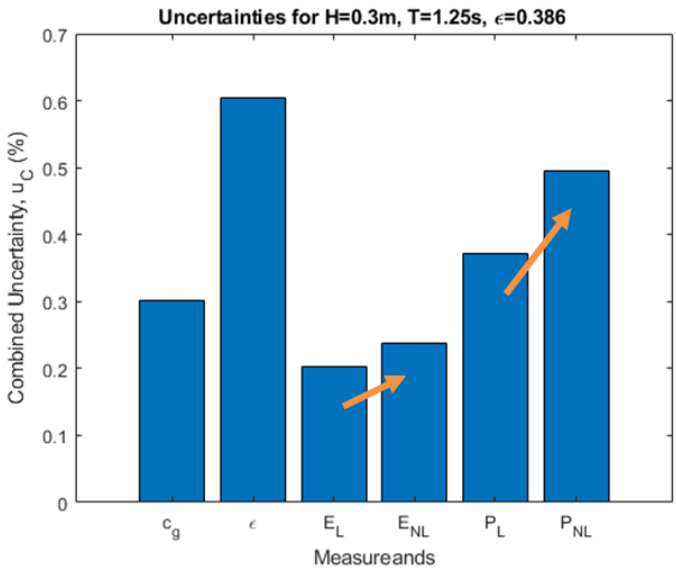


*Figure 16: Large wave steepness and thus nonlinearity causes slightly more uncertainty in the nonlinear estimations of energy and power.*

A major point of uncertainty is not in the measurements but in the calculation of regular wave power. The vast majority of WEC research utilizes linear wave assumption rather than the full nonlinear solution for energy flux. For the wave condition in Figure 16, the linear estimation of wave power was 107 W/m (nominally), and the nonlinear estimation was 95 W/m (nominally). This is an 11% difference, larger than the expanded uncertainty of +/- 3%. Using the linear assumption causes an overestimation of wave power, and thus will cause an underestimation of capture width ratio.

Finally, Figure 17 shows the expanded uncertainty, U, which is the 95% confidence interval of the incident power estimation. Overall, the 4 regular wave conditions in this experiment had less than +/- 2.5% uncertainty in the incident wave power. This work will be used to propagate uncertainty to capture width ratio when the uncertainty analysis in the WEC power is complete.

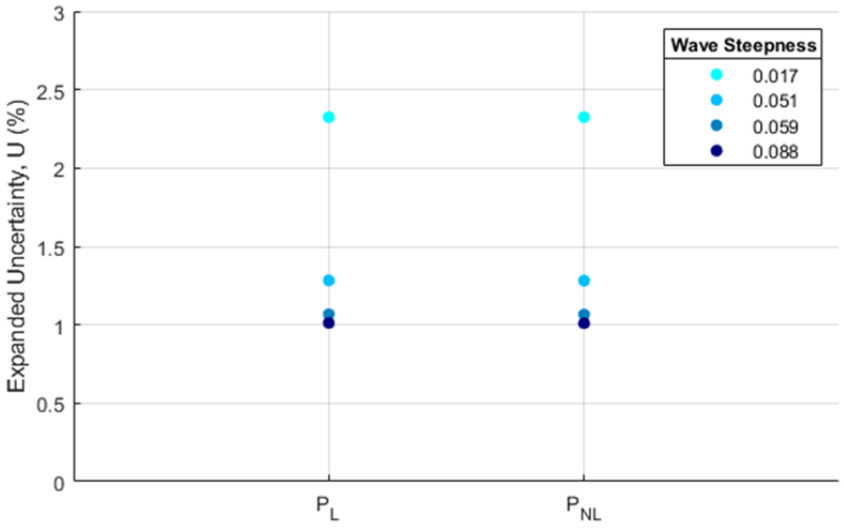


*Figure 17: Expanded uncertainty of linear and nonlinear incident wave power. The linear and nonlinear have the same uncertainty. Overall, this experiment produced less than +/- 2.5% uncertainty in the incident wave power. Wave steepness has nondimensional units of m/m.*

## 7.2 Lesson Learned and Test Plan Deviation

*General Lessons Learned*

The O.H. Hinsdale Wave Research Laboratory had recently commissioned a new flap wavemaker and this TEAMER testing was the first to utilize the wavemaker at this water depth. The TEAMER testing provided a great opportunity for the applicant and the facility to find the limits of the flume and the wave maker. For example, the desired water depth of 4 m could not be achieved given the physical limitations of the tank (communication and drainage location conflicts at 4m). This limitation was not trivial and could not be avoided for this testing, thus the wave conditions, mooring design, and deployment procedure were adapted. This could not be avoided for this testing but subsequent TEAMER testing at Hinsdale with the new wavemaker have already benefitted from this learning. There was also a learning curve for the applicant and the facility to understand the programming for the flap wave maker which is inevitable for a new system. This TEAMER testing has ultimately made testing more efficient and effective for the future.

Previously, we used turnbuckles to tension the mooring lines. The turnbuckles were heavy, time-consuming, and required installation from a kayak in the water. We switched to winches with straps that were hard mounted to the flume and can be tensioned from the dry outside the flume which is safer, faster, and easier.

The default recommended settling time for the flume is 20 minutes between tests to return to quiescent conditions. This is necessary in some wave conditions, but limits the number of tests possible during a day. To remedy this, all wave conditions were run once at the very beginning of testing and analysis was completed to identify the settling time to return to quiescent conditions. This resulted in settling time being reduced by several minutes for all conditions. In the end, saved 8 hours of testing, improved efficiency, and allowed for more tests to be completed.

Underwater lights are convenient for visualizing testing and capturing high-quality photos and videos, especially in such deep water. We only used them towards the very end of testing but will be implementing them more in the future.

Each test facility has a unique wave period at which natural resonance occurs that causes undesired cross-waves or "wing" based on the width of the flume. For the O.H. Hinsdale Wave Research Laboratory Large Wave Flume, this occurs at about 1.5 s (0.65 Hz). This sloshing behavior is important to know before testing and consider when analyzing the results.

*Deviations from the System Identification Test Plan*

There were two minor deviations from the original test plan. First, we only used white noise spectra for the force actuation signal (instead of the mentioned pink noise) since LUPA has near perfect actuation resulting in clean signals. Second, we started the frequency band for the pink noise wave maker at 0.1Hz instead of 0.05Hz due to practical reasons. The 0.05Hz corresponds to a 20s wave, which has a wavelength of about two orders of magnitude higher than LUPAs characteristic dimension, i.e., no hydrodynamic significance.

*Deviations from the Uncertainty Test Plan*

The wave conditions were downselected from the original test plan for several reasons. Some of the conditions caused the wave maker to clip a significant portion of the irregular wave spectrum due to its physical limitations. The small wave heights and longer periods produced little response in the two-body six-DOF LUPA configuration and were unable to produce high-quality power data. It was also determined that the wave conditions should be run with and without LUPA in the tank for better uncertainty analysis of undisturbed incident wave power, limiting the time to run additional conditions.

*Table VI: Regular wave conditions*

| Wave Period (s) | Wave Height (m) | PTO Damping (N/(m/s)) | PTO Stiffness (N/(m/s)) |
|---|---|---|---|
| **1.75** | 0.10 | 1800 | -300 |
| **1.75** | 0.15 | 1800 | -300 |
| **2.35** | 0.05 | 3200 | 1600 |
| **2.35** | 0.15 | 3200 | 1600 |

*Table VII: Irregular wave conditions, Pierson-Moskowitz*

| Peak Period (s) | Significant Wave Height (m) | PTO Damping (N/(m/s)) | PTO Stiffness (N/(m/s)) |
|---|---|---|---|
| **1.75** | 0.08 | 1800 | -300 |
| **1.75** | 0.10 | 1800 | -300 |
| **2.35** | 0.08 | 3200 | 1600 |
| **2.35** | 0.12 | 3200 | 1600 |

The tables above show the regular and irregular waves used in this testing campaign. These specific wave periods were chosen after system identification revealed 1.75 s as a resonance period and 2.35 s as a period of interest to compare to the resonance. The regular waves were repeated for 10 trials with, and without, LUPA for a total of 20 trials per condition, following the ITTC guidelines [17]. Each trial had at least 20 regular wave cycles. The irregular waves had a repeat period of 300 s and were repeated 2.5 times for each trial. Each wave condition was repeated for 5 trials with and without LUPA for a total 10 trials per condition. The PTO damping and stiffness were determined through impedance matching and kept constant over the trial.

# 8 Conclusions and Recommendations

The conclusions section is divided into two parts that match the project objectives: system identification and uncertainty.

*System Identification*

System identification was performed using data from a set of open-loop experimental tests. A set of linear non-parametric models produced by this analysis. A multi-input, single-out models, in which wave amplitude and actuator force are used to predict motion of the PTO, were produced – this style of analysis represents a novel accomplishment and will be further documented in a peer-reviewed article. Generally, the models are consistent between tests, but do show some nonlinearity. These models were subsequently validated against a set of experiments not used in fitting the models. The validations show good agreement between the models and the experimental data.

*Uncertainty*

The goals of uncertainty testing were to collect data on regular and irregular waves and estimate uncertainty for common wave energy converter performance metrics. Regular and irregular conditions were tested to compare varying degrees of wave nonlinearity and its effects on uncertainty. The initial analysis presented here finds that smaller wave heights have larger uncertainty percentages likely due to the sensor signal-to-noise ratio. This work also showed that propagating uncertainties of wave height, period, density, gravity, and water depth through a Monte Carlo Method found combined and expanded uncertainty of wave power to be under +/- 2.5% for the tested conditions. An important source of uncertainty is the difference between the linear and nonlinear calculations of incident regular wave power. For a wave condition of high steepness, and thus nonlinearity, the linear calculation overestimated the full nonlinear solution by 11%, which would cause underestimations in the capture width ratio. Future analysis includes processing the irregular wave data and propagating uncertainty into the frequency domain.

A reflection analysis was also completed which suggests running longer trials that include small, reflected waves may reduce uncertainty and improve efficiency in the testing campaign. For example, instead of running multiple short trials that only collect data on the initial undisturbed waves which causes more transition and settling time, one could run longer trials to achieve repetition or complete longer duration tests like PTO control studies or system identification without concern that it will introduce more uncertainties in the waves. This is very wave and tank-dependent so future work in this area could extend these methods to different wave conditions and testing facilities.

# 9 ACKNOWLEDGEMENTS

The success of this project was fundamentally dependent on collaboration between OSU, Hinsdale and SNL staff. The authors acknowledge the invaluable input from Dr. Bret Bosma, Dr. Pedro Lomonaco, and Dr. Tim Maddox from OSU & Hinsdale, and Dr. Ryan Coe, Dr. Giorgio Bacelli, Dr. Domonic Forbush from Sandia National Laboratories.

# 10 REFERENCES

[1] D. D. Forbush, G. Bacelli, and R. G. Coe, "Self-Tuning, Load-Mitigating Feedback Control of a 3-DOF Point Absorber," *Int. Mar. Energy J.*, vol. 5, no. 1, pp. 23–35, 2022, doi: 10.36688/imej.5.23-35.

[2] G. Bacelli, R. G. Coe, D. Patterson, and D. Wilson, "System identification of a heaving point absorber: Design of experiment and device modeling," *Energies*, vol. 10, no. 472, pp. 1–33, 2017, doi: 10.3390/en10040472.

[3] D. D. Forbush, G. Bacelli, S. J. Spencer, R. G. Coe, B. Bosma, and P. Lomonaco, "Design and testing of a free floating dual flap wave energy converter," *Energy*, vol. 240, no. 122485, pp. 1–12, 2022, doi: 10.1016/j.energy.2021.122485.

[4] G. Bacelli, S. J. Spencer, D. C. Patterson, and R. G. Coe, "Wave tank and bench-top control testing of a wave energy converter," *Appl. Ocean Res.*, vol. 86, no. December 2017, pp. 351–366, 2019, doi: 10.1016/j.apor.2018.09.009.

[5] H. Cho, G. Bacelli, and R. G. Coe, "Model Predictive Control Tuning by Inverse," *Energies*, vol. 12, no. 4158, pp. 1–18, 2019, doi: 10.3390/en12214158.

[6] G. Bacelli, V. Nevarez, R. G. Coe, and D. G. Wilson, "Feedback Resonating Control for a Wave Energy Converter," *IEEE Trans. Ind. Appl.*, vol. 56, no. 2, pp. 1862–1868, 2020, doi: 10.1109/TIA.2019.2958018.

[7] D. G. Wilson, R. D. Robinett III, G. Bacelli, O. Abdelkhalik, and R. G. Coe, "Extending Complex Conjugate Control to Nonlinear Wave Energy Converters," *J. Mar. Sci. Eng.*, vol. 8, no. 84, pp. 1–21, 2020, doi: 10.3390/jmse8020084.

[8] G. Bacelli and R. G. Coe, "Comments on Control of Wave Energy Converters," *IEEE Trans. Control Syst. Technol.*, vol. 29, no. 1, pp. 2020–2023, 2021, doi: 10.1109/TCST.2020.2965916.

[9] R. G. Coe, G. Bacelli, and D. Forbush, "A practical approach to wave energy modeling and control," *Renew. Sustain. Energy Rev.*, vol. 142, no. May 2021, p. 110791, 2021, doi: 10.1016/j.rser.2021.110791.

[10] Specialist Committee on Uncertainty Analysis of 25th ITTC, "Guide to the Expression of Uncertainty in Experimental Hydrodynamics," 2008.

[11] ITTC, "ITTC recommended guidelines: wave energy converter model test experiments," *Proc. 28th Int. Towing Tank Conf.*, vol. 7.5-02–07, pp. 1–17, 2017.

[12] J. Orphin, J. Nader, and I. Penesis, "Uncertainty analysis of a WEC model test experiment," *Renew.*

*Energy*, vol. 168, pp. 216–233, 2021, doi: 10.1016/j.renene.2020.12.037.

[13] J. Orphin, I. Penesis, and J.-R. Nader, "Uncertainty Analysis for a Wave Energy Converter: the Monte Carlo Method," *AWTEC 2018 Proc.*, pp. 1–10, 2018.

[14] J. Orphin, J. Nader, I. Penesis, and D. Howe, "Experimental Uncertainty Analysis of an OWC Wave Energy Converter," *Eur. Wave Tidal Energy Conf.*, no. August, pp. 1–11, 2017.

[15] R. Pintelon and J. Schoukens, "System Identification: A Frequency Domain Approach," in *Encyclopedia of Systems and Control*, Hoboken, NJ, USA: John Wiley & Sons, 2012, pp. 469–479.

[16] J. M. Fornies-Marquina, J. Letosa, M. Garcia-Gracia, and J. M. Artacho, "Error Propagation for the Transformation of Time Domain into Frequency Domain," *IEEE Trans. Magn.*, vol. 33, no. 2, pp. 1456–1459, 1997, doi: 10.1109/20.582534.

[17] Specialist Committee on Testing of Marine Renewable Devices of the 28th ITTC, "Uncertainty Analysis for a Wave Energy Converter," 2017.

[18] International Electrotechnical Commission, "IEC/TS 62600-100, Marine energy – Wave, tidal and other water current converters – Part 100: Electricity producing wave energy converters – Power performance assessment," Geneva, Switzerland, 2012.

[19] A. Mohtat, S. C. Yim, and A. R. Osborne, "Energy Content Characterization of Water Waves Using Linear and Nonlinear Spectral Analysis," *J. Offshore Mech. Arct. Eng.*, vol. 144, no. 1, 2022, doi: 10.1115/1.4051860.

[20] International Electrotechnical Commission, "IEC TS 62600-103 Marine energy – Wave, tidal and other water current converters – Part 103: Guidelines for the early stage development of wave energy converters – Best practices and recommended procedures for the testing of pre-prototype devices," Geneva, Switzerland, 2018.

# 11 APPENDIX

## ○ APPENDIX A – ADDITIONAL DATA ACQUISITION

Additional details on the measurements can be found in Table VIII.

*Table VIII: Data Acquisition Channels and Sensors*

| Sensor Name | Quantity | DAQ System | Physical Quantity | Units |
|---|---|---|---|---|
| **Load cell** | 4 | Hinsdale | Mooring line tension | Newtons |
| **Wave gage** | 4 | Hinsdale | Free surface elevation | Meters |
| **String pot** | 1 | Hinsdale | Relative motion of spar to tank | Meters |
| **Draw wire** | 1 | Onboard LUPA | Relative motion of spar and float | Meters |
| **Load cell** | 2 | Onboard LUPA | Force in PTO | Newtons |
| **Vertical Reference Unit** | 1 | Onboard LUPA | Accelerations, angular position, angular velocity | Meters per seconds squared, radians, radians per second |
| **Temperature Sensor** | 1 | Onboard LUPA | Motor temperature | Degrees Celsius |
| **Encoder** | 1 | Onboard LUPA | Motor position | Radians |
| **Motor Drive** | 1 | Onboard LUPA | Motor torque, motor current | Newton-meters, amps |